Geotextiles and Geomembranes 49 (2021) 1312–1323

Contents lists available at ScienceDirect

Geotextiles and Geomembranes

journal homepage: www.elsevier.com/locate/geotexmem

Critical length of encased stone columns

Marina Miranda [a,*], Jesús Fernández-Ruiz [b], Jorge Castro [a]

[a] Department of Ground Engineering and Materials Science, University of Cantabria, Santander, Spain
[b] Department of Civil Engineering, University of La Coruña, La Coruña, Spain

ARTICLE INFO

Keywords:
Geosynthetics
Geotextiles
Encased stone columns
Critical length
Settlement
Footing
Finite element analyses

ABSTRACT

Encased stone columns are vertical inclusions in soft soils formed by gravel wrapped usually with a geotextile. Their critical length is the one where further lengthening of the column provides a negligible improvement and it is therefore not effective to build columns longer than it. This paper aims to obtain common values of the critical length using simplified two-dimensional axisymmetric and full three-dimensional finite element analyses. A uniform soft soil layer with a linear elastic perfectly plastic behaviour is considered for the sake of simplicity. For the studied cases, the critical column length is around 1.3–2.5 times the footing diameter for encased stone columns, and slightly lower for ordinary stone columns, namely around 1.1–1.9. The critical length of the encasement is found to be slightly lower than the critical column length. The value of the critical column length is related to the extent of plastic deformation and that may be used to decide the column length in the design phase without the need of parametric analyses. As a first approximation, a general value of the critical column length of 2 and 2.5 times the footing diameter may be considered for ordinary and encased stone columns, respectively.

1. Introduction

Ground improvement using stone columns is a popular technique to improve soft soils for foundation of embankments or structures (e.g., Al Ammari and Clarke, 2018; Barksdale and Bachus, 1983; Bong et al., 2020; Etezad et al., 2018; Kirsch and Kirsch, 2010; Han, 2015; Hosseinpour et al., 2019; Lima et al., 2019; Ong et al., 2018; Siahaan et al., 2018). In very soft soils, ordinary stone columns may not be suitable because of the lack of lateral confinement ($c_u \leq 5-15\ kPa$) (e.g., Wehr, 2006). In those cases, encasing the columns with geotextiles or other geosynthetics has been a successful solution in recent years (e.g., Alexiew and Raithel, 2015; Alkhorshid et al., 2019; Almeida et al., 2019; Cengiz and Güler 2018; Ehsaniyamchi, and Ghazavi, 2019; King et al., 2018; Li et al., 2020; Nagula et al., 2018; Schnaid et al., 2017).

Ordinary stone columns (OSC) and encased stone columns (ECS) may reach a rigid substratum (end-bearing columns) or may be embedded just on a soft soil layer (floating columns). For the latter case, the length of the columns is an important design parameter to be chosen. In some cases, it may be more cost-effective to add additional columns than increasing the length of the columns. In this way, the concept of the critical length of stone columns appears. It is the column length where further lengthening of the column provides a negligible improvement (e.g., settlement reduction) and it is therefore not effective to build columns longer than it. For columns longer than the critical length, the improvement achieved with stone columns does not notably change or increase. Although the load transfer mechanisms and the reasons for the critical length are different from piles, the meaning of the concept of critical length is equivalent (e.g., Fleming et al., 2009).

Although there are several proposals for the critical length of the columns (L_{cr}), the available information could be confusing as detailed in the next section. Besides, the topic is marginally treated as a part within more general papers. To the best of the authors' knowledge, this is the first paper specifically devoted to the critical length of ESC. Detailed and comprehensive numerical analyses are presented to evaluate the critical column length and parametric analyses are presented, providing guidance for future designs.

A literature review is first presented in Section 2, summarizing the different proposals for L_{cr}; next, the numerical models for the proposed study are presented in Section 3 and the results and their discussion are covered in Section 4. In Section 5, partially encasing the column is studied. The paper concludes with the theoretical justification for L_{cr} and design recommendations (Section 6) and the conclusions.

* Corresponding author. Group of Geotechnical Engineering, Department of Ground Engineering and Materials Science, University of Cantabria, Avda. de Los Castros, s/n, 39005, Santander, Spain.
E-mail addresses: mirandama@unican.es (M. Miranda), jesus.fernandez.ruiz@udc.es (J. Fernández-Ruiz), castrogj@unican.es (J. Castro).

https://doi.org/10.1016/j.geotexmem.2021.05.003
Received 28 January 2021; Received in revised form 30 April 2021; Accepted 4 May 2021
Available online 30 May 2021

Notation

a_r	Area replacement ratio: $a_r = A_c/A_l$
c	Cohesion
d_c	Column diameter
K_0	Coefficient of lateral pressure at rest
p_{app}	Uniform applied vertical pressure
s	Centre-to-centre column spacing
s_z	Settlement
s_{z0}	Settlement without columns
x,y,z	Cartesian coordinates
A	Cross-sectional area
B	Footing width
D	Footing diameter
E	Young's modulus
E_m	Oedometric (constrained) modulus: $E_m = [E(1-\nu)]/[(1+\nu)(1-2\nu)]$
H	Soft soil layer thickness
J_g	Encasement stiffness
L	Column length
L_g	Encasement length
L_{cr}	Critical column length
$L_{g,cr}$	Critical encasement length
β	Settlement reduction factor: $\beta = s_z/s_{z0}$
γ'	Effective unit weight
ν	Poisson's ratio
φ	Friction angle
ψ	Dilatancy angle

Subscripts / superscript

c,s,g,l	column, soil, encasement, loaded area

2. Literature review

Hughes and Withers (1974) seem to be the first authors to study the critical length of OSC using laboratory tests. They used small scale laboratory tests and a footing diameter (D) equal to that of the column (d_c). They found that a bulging zone was developed in the upper part and proposed $L_{cr} = 4D$. Since then, several authors have studied its value. A review of these different proposals for L_{cr} may be found in Table 1 and, for example, in Babu et al. (2013) for OSC. The values show some range of variation and, in many cases, they are given as a function of d_c, but in others, as a function of the footing width or diameter (B or D, respectively).

Castro (2014) for OSC and Castro (2017a) for ESC showed that the column length to diameter ratio (L/d_c) (slenderness of the column) has a minor influence (second order effect) on the ground improvement achieved with stone columns and the ratio L/B plays a major role. Hence, L_{cr} should be better expressed in terms of the footing dimensions (B or D). The source of confusion could be that for piles the critical length is given as a function of the pile diameter, i.e. the slenderness ratio (e.g., Fleming et al., 2009), and that in the original proposal by Hughes and Withers (1974), D happened to be the same as d_c.

A reanalysis of the values shown in Table 1 in terms of D or B instead of d_c provides reasonable values and a narrower range of variation for the critical column length. For example, in McKelvey (2002), $d_c = 25$ mm, $D = 100$ mm, $L_{cr} = 150$ mm, and then, $L_{cr} = 1.5\ D$; in Najjar et al. (2010), $d_c = 20$ mm, $D = 71$ mm, $L_{cr} = 120$ mm, and then, $L_{cr} = 1.7\ D$. The precision of the critical length obtained from some laboratory tests is limited because few column lengths are normally tested.

Muir Wood et al. (2000) pointed out the importance of the deformation mechanism beneath the footing. Castro (2017b) conceptually showed that the critical column length for bearing capacity depends on the failure mechanism (Fig. 1a) and the critical column length for settlement reduction is related to the extension of the pressure bulb beneath the footing (Fig. 1b). Since the critical length is larger for settlement reduction, this is the one that is normally used. The pressure bulb is a useful concept, but it is strictly only valid for an elastic behaviour, which is not usually the case for an efficient design of OSC or ESC. Castro et al. (2019) showed that the critical column length is related to the extension of plastic deformation in the soil and column (Fig. 1c).

The concept of critical column length is useful only for footings or small groups of columns because for large loaded areas (e.g., embankments), the critical length is larger than the soft soil layer thickness and then, there is no critical length in practise (e.g., Yoo, 2010).

Table 1
Values of the critical column length. Literature review.

Reference	*Column*	*Type*	S/G[c]	a_r (%)	L_{cr}	$L_{cr} = f(D)$[a]
Black et al. (2011)	OSC	Lab.	S/G	17–40	8-10 d_c	3.3–4.3 D
Dash and Bora (2013)	OSC	Lab.	S[b]	44	≤5 d_c	≤3.3 D
Hughes and Withers (1974)	OSC	Lab.	S	100	4 d_c	4 D
Malarvizhi and Ilamparuthi (2007)	OSC/ESC	Num.	S	19	7.5 d_c	3.2 D
McKelvey (2002)	OSC	Lab.	G	24	6 d_c	1.5 D
Muir Wood et al. (2000)	OSC	Lab.	G[b]	10–30	1.5 B	
Najjar et al. (2010)	OSC	Lab.	S	8–18	6 d_c	1.7 D
Ng (2017)	OSC	Num	G	20–70	1.2–2.2 D	
Remadna et al. (2020)	OSC	Num	G	18–36	1.2–2 D	
Tan et al. (2014)	OSC	Num	G	20–70	1.3-2 D	
Wehr (2004)	OSC	Num.	G	58	1.7 D	
Zhou et al. (2017)	OSC	Num.	G	10–40	2 B	

Lab.: Laboratory tests; Num.: Numerical analyses.
[a] Reanalysis proposed here.
[b] Additional columns outside the footing.
[c] Single (S) or group (G) of columns (S/G).

3. Numerical models

Finite element analyses, using the Plaxis codes (Brinkgreve et al., 2018, 2019), were performed to study the critical column length. Additionally, the critical encasement length was also analysed. Both two-dimensional (2D) and three-dimensional (3D) models were considered. The study started with a simple reference case and parametric studies were performed to analyse the influence of several parameters on the critical column length.

3.1. Basic assumptions

The soft soil and the stone columns were modelled as continuum elements and the geosynthetic encasement was modelled as an element that has only normal stiffness, i.e. it only has translational degrees of freedom at their nodes and can only sustain tensile stresses. The bottom boundary was fixed and roller vertical conditions were assumed for the lateral boundaries.

Perfect bonding between soil, columns and their encasements at their interfaces was modelled, as it is common practice (e.g., Keykhosropur et al., 2012), because they are tightly interlocked. The rigid footing was

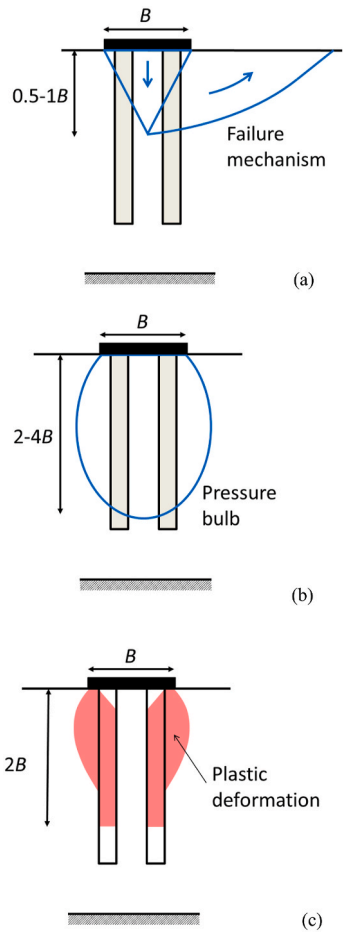

Fig. 1. Justification of critical column length in a homogeneous soil layer: (a) Bearing capacity; (b) Settlement reduction in elastic materials linked to pressure distribution; (c) Settlement reduction in elasto-plastic materials related to plastic deformation.

assumed as perfectly rough and modelled as a very stiff plate ($EA = 10^{10}$ kN/m and $EI = 10^{12}$ kN m^2/m) that produces uniform settlements.

All the numerical simulations were performed using a small strain formulation. The footing, the geosynthetic encasement and the column were "wished-in-place", ignoring the changes in the natural soil due to column construction, such as for example in soil stiffness and in K_0 (e.g., Castro and Karstunen, 2010). Drained conditions were assumed for all the process, i.e. no excess pore pressures were generated. Geostatic initial stresses were generated using the effective soil unit weight (γ') and the coefficient of lateral earth pressure at rest, $K_0 = 0.6$. For simplicity, the ground water level was assumed to be at the ground surface and an effective unit weight of $\gamma' = 10$ kN/m^3 for soil and column was directly considered without modelling pore water pressures. The applied pressure on the footing, p_{app}, is 100 kPa for the reference case.

3.2. 2D models

Plaxis 2D 2019 (Brinkgreve et al., 2019) was used to represent a simplified 2D axisymmetric model of only one centered column beneath a rigid circular footing. This 2D simplified model reproduces similar values of the footing settlement than those of a full 3D model of a group of columns with the same area replacement ratio and the same ratio between the encasement stiffness (J_g) and the column diameter (Castro, 2017a). The concentric ring approach (e.g., Castro, 2017b; Ng, 2017) would be better to consider the location of the columns but it is not clear how to model the confinement effect of the geotextile encasement. As this work is focused on ESC, it was decided to use the single central column approach. The area replacement ratio (a_r) is the ratio between the area of the columns and the loaded area, i.e. footing area in this case.

For the reference case, the footing diameter, D, is 2.5 m and the column diameter (d_c =1.37 m) was chosen to give an area replacement ratio of $a_r = 30\%$. The soil profile was simplified to only one homogeneous soil layer, with a thickness of $H = 10$ m (Fig. 2). Both the soil and column were modelled as linear elastic-perfectly plastic materials using the Mohr-Coulomb yield criterion and a non-associated flow rule ("Mohr-Coulomb model"). Common values were chosen for the soil and column parameters (Table 2). A stiffness of $J_g = 2$ MN/m was taken for the geosynthetic encasement and a null Poisson's ratio ($\nu_g = 0$) because the geosynthetic encasement was assumed to have two major directions (radial and longitudinal), which behave independently (e.g., Soderman and Giroud, 1995; Castro, 2016).

The column length was varied from $L = 10$ m (end-bearing column, $L/H = 1$) to $L = 0$ m (no column) in steps of 0.5 m. The critical column length was identified from the variation of the settlement reduction factor with the column length. The settlement reduction factor (β) is the ratio between the settlement with columns and the settlement without columns (s_z/s_{z0}). Parametric analyses were performed using the reference case and varying the value of the parameters as shown in Table 3. The case with $J_g = 0$ is equivalent to no-encasement (OSC) and all the parametric analyses were performed for both ESC and OSC.

From the calculations, some mesh sensitivity (of around 3%) was observed between different cases, but the same mesh was used to identify each critical column length, i.e. for each case with different column lengths (Fig. 2).

3.3. 3D models

The 2D models have been complemented with 3D analyses using Plaxis 3D 2018 (Brinkgreve et al., 2018) for verification purposes, i.e. to check that the critical column length and the trends observed with the 2D model are the same for the corresponding 3D cases.

Equivalent cases only to the 2D reference case were modelled in 3D. A square footing with the same area as the 2D footing, i.e. $B = 2.21$ m, was considered. Four columns beneath the footing were modelled and their diameter $d_c = 0.68$ m was chosen to have the same area replacement ratio as that in the 2D reference case, i.e. $a_r = 30\%$. The encasement stiffness (J_g=1 MN/m) was again chosen to have the same J_g/d_c ratio as that in the 2D reference case. OSC, i.e. $J_g = 0$, were also simulated. The same single homogeneous soil layer of $H = 10$ m was modelled and the soil and column properties were the same (Table 2). Due to symmetry, only one quarter of the model was numerically represented (Fig. 3).

The column length was also varied from $L = 10$ m (end-bearing column, $L/H = 1$) to $L = 0$ m (no column) in steps of 0.5 m and column length vs. settlement reduction curves were plotted to get the critical column length. The spacing between the columns was varied (s=0.9, 1.2

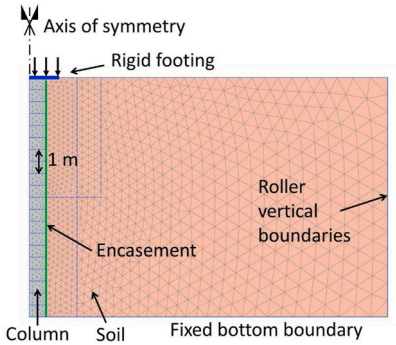

Fig. 2. 2D finite element model. Reference case.

Table 2
Soil and column properties for the reference case.

Material	*E*(MPa)	ν(-)	*c*(kPa)	φ(°)	ψ(°)	γ_{sat}(kN/m^3)
Soil	2	0.33	5	25	0	20
Column	30	0.33	0.1	45	10	20

Table 3
Summary of parametric analyses.

Parameter	Values
a_r[a]	10, **30**, 50, 70, 100%
J_g	**0**, 0.5, 1, **2**, 3, 4, 5 MN/m
c_s, φ_s	(3, 23) (**5, 25**) (7, 27) (9, 29) (11, 31) (kPa, °)
φ_c, ψ_c	(35, 0) (40, 5) (**45, 10**) (50, 15) (°, °)
p_{app}	20, **100**, 200 kPa
D[b]	1, 2, **2.5**, 3 m
H	7.5, **10**, 12.5, 15, 17.5, 20
E_s	0.5, 1, **2**, 5 MPa
E_c	10, **30**, 80 MPa

In boldface: values of the reference case.
[a] Varying d_c and J_g, keeping constant J_g/d_c ratio.
[b] Also varying, d_c, J_g and p_{app} to keep constant a_r, J_g/d_c and $p_{app}/(\gamma D)$ ratios.

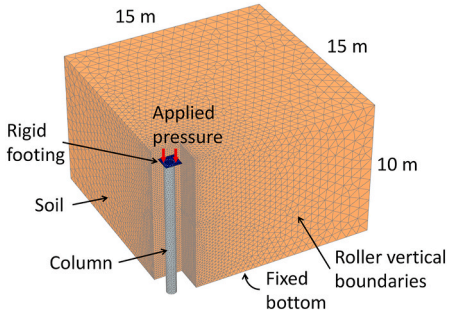

Fig. 3. 3D finite element model ($s = 1.25$ m). Encasement and soil surrounding the column are not shown for visualization of the column.

and 1.5 m) (Fig. 4) to study its influence in the critical column length. It is worth noting that varying the spacing between the columns here does not imply changing a_r, and it only changes the column relative position within the footing.

In the 3D calculations, some mesh sensitivity was observed (less than 3% for the simulated cases), but again the same mesh was used to identify each critical column length, i.e. for each case with different column lengths (Fig. 3).

4. Results and discussion

The results of the parametric study are presented in the following. For each case, the variation of the settlement reduction with the column length was obtained. This variation, which shape is similar to an "S", was interpreted to obtain L_{cr}. The procedure to determine L_{cr} was to fit

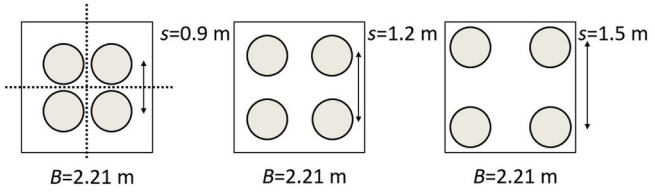

Fig. 4. Variation of column relative position in the 3D model (only one quarter was modelled).

two lines to the two straight parts of the data obtained and the intersection of both lines provides the value of L_{cr} (Fig. 5). The procedure is somehow analogous to the obtention of the end of primary consolidation in a consolidation curve using Casagrande's method. For each straight part, a linear regression was performed using the least minimum square procedure and to be consistent, both lines were fitted, when possible, to the same ranges of values, namely the 4 values between 0.6 and 1.2 L/D and the 4 values in the range 2.4 and 3 L/D.

4.1. Area replacement ratio

The area replacement ratio is usually the key parameter in a stone column treatment. Here, it was varied between 10% and 100%, varying the column diameter (d_c) and keeping the same footing dimensions ($D =$ 2.5 m). On the other hand, the influence of the encasement is controlled by its stiffness, or more precisely, by the J_g/d_c ratio. Therefore, J_g was also varied to keep the J_g/d_c ratio constant. The settlement for the unimproved soil is approximately $s_{z0} = 12.3$ cm. Fig. 6a portrays the results for ESC and Fig. 6b for OSC. As expected, lower settlements are obtained for encased columns, larger area replacement ratios and longer columns. In addition, Fig. 6 clearly shows that there is a critical column length (L_{cr}), beyond which the settlement reduction is small. For OSC, the settlement reduction beyond L_{cr} is not visible, while for ESC, there is a minor reduction of the settlement (this reduction is minor because mainly elastic strains exist as explained in Section 6).

The critical column length is larger for ESC than for OSC (Fig. 7) as expected, because ESC transfer the applied stresses deeper into the ground. Additionally, for ESC, the critical length decreases with a_r, while this variation is negligible for OSC. Muir Wood et al. (2000) argued that, for higher a_r, the pressure bulb (Fig. 1b) should be deeper because the average stiffness is larger. Tan et al. (2014) found larger critical (optimum) lengths for higher a_r and OSC using finite element simulations. However, as analysed in detail in Section 6, for ESC the influence of plastic strains is the controlling mechanisms (Fig. 1c), and then, for larger a_r, the extension with depth of the plastic strains is shorter, which justifies the lower value of L_{cr} with a_r.

4.2. Encasement stiffness

The encasement stiffness (J_g) is also a decisive parameter for ESC. It was varied between 0 (i.e. no encasement, OSC) and 5 MN/m to cover a wide range of values used in practice (e.g., Alexiew and Raithel, 2015). As already known, the settlement is further reduced for stiffer encasements (Fig. 8). Interestingly, for short columns, namely $L/D < 1$, the encasement has a negligible influence on the settlement reduction. This is because, in short columns, the settlement occurs mainly by punching of the column tip and lateral bulging of the column is negligible. Therefore, encasing the column is not useful in those cases.

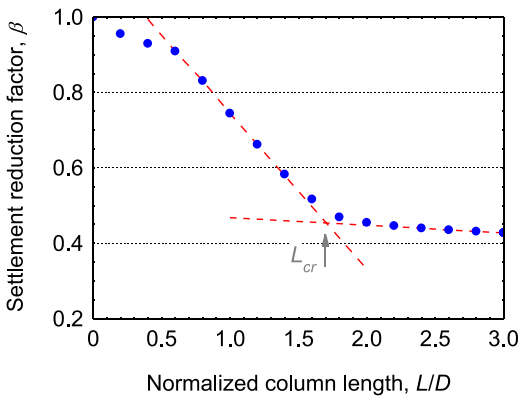

Fig. 5. Procedure to determine L_{cr}. Reference case for encased columns.

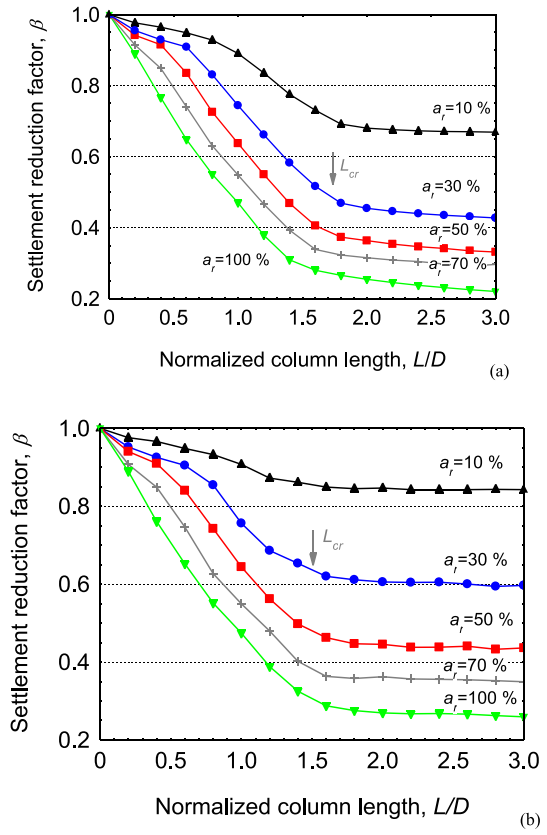

Fig. 6. Variation of the settlement reduction with normalized column length for different area replacement ratios: (a) ESC; (b) OSC.

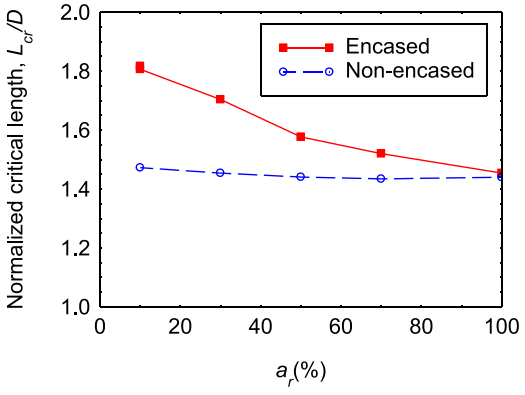

Fig. 7. Normalized critical column length for different area replacement ratios.

Nevertheless, those cases are not recommended for design.

The critical column length increases with J_g, because the vertical stresses are transferred deeper into the original soft soil. Fig. 9 shows that the critical column length is clearly larger for ESC than for OSC, as already shown in Fig. 7. In Fig. 9, the influence of the geotextile stiffness is more noticeable in cases with smaller a_r because the encasement contribution is controlled by the J_g/d_c factor and in this study, the changes in the area replacement ratio have been simulated by varying the diameter of the column. Consequently, smaller a_r, values correspond to smaller column diameters and better confinement provided by the encasement.

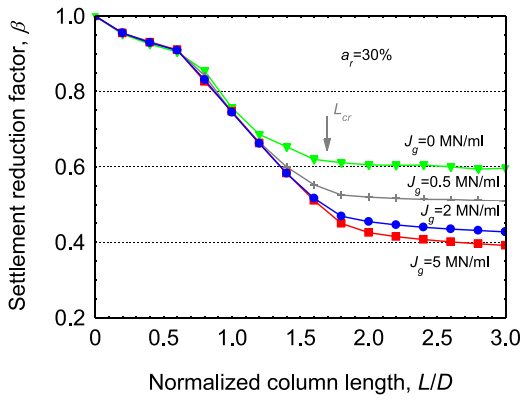

Fig. 8. Variation of the settlement reduction with normalized column length for different encasement stiffnesses.

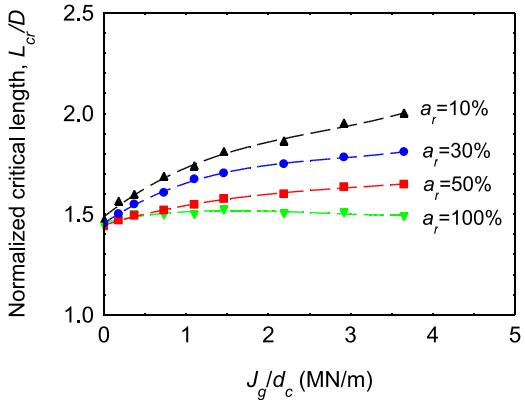

Fig. 9. Critical column length for different encasement stiffnesses (normalized) and area replacement ratios.

4.3. Soft soil strength

For the applied load in the reference case (p_{app} = 100 kPa), significant plastic strains are developed in the soft soil. Thus, the settlement of the footing decreases with an increase in the soft soil strength. For example, the settlement of the footing without column decreases from s_{z0} = 12.3 cm for the reference case, i.e. c_s = 5 kPa and φ_s = 25°, to s_{z0} = 8.35 cm for the case with c_s = 11 kPa and φ_s = 31°. As already done for a_r and J_g, the variation of the settlement reduction is plotted against the column length for different soft soil strengths (Fig. 10) to study the influence of the soft soil strength on the critical column length. In Fig. 10, the normalized value of the settlement, i.e. the settlement reduction, is plotted. This means that for each soft soil strength the settlement is normalized by different s_{z0} values. For brevity, only the soft soil friction angles are depicted in the figure, but they also imply changing the soft soil cohesion accordingly (please, refer to Table 3).

The improvement achieved with the column treatment is usually larger for a softer soil (Fig. 10), but for short columns (L/D < 1), which are not recommended for design. For the largest soil strength (namely, c_s = 11 kPa and φ_s = 31°), the location of the critical column length is not so apparent because the transition between column lengths where the settlement is clearly reduced and those where it is not is smooth and elastic strains get noticeable.

The critical column length progressively decreases with the soft soil strength (Fig. 11), for example, for ESC from L_{cr} = 2D for (c_s = 3 kPa and φ_s = 23°) down to L_{cr} = 1.4D for (c_s = 11 kPa and φ_s = 31°). The variation for OSC and ESC is similar and, in both cases, tends to a similar asymptotic value. This variation is related to the extension of the plastic

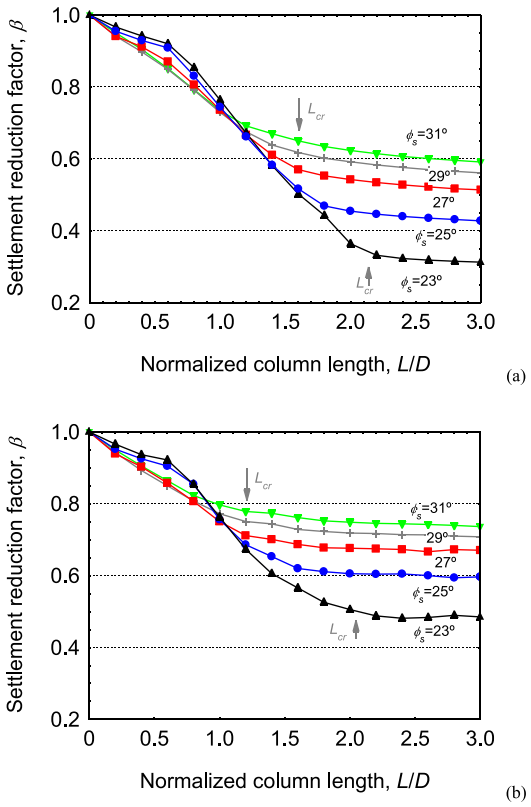

Fig. 10. Variation of the settlement reduction with normalized column length for different soil strengths: (a) ESC; (b) OSC.

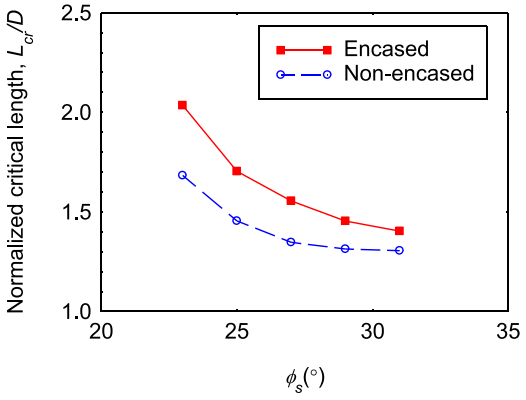

Fig. 11. Critical column length for different soft soil strengths.

zone (Fig. 1c) as it will be shown in Section 6. On the other hand, the asymptotic value is related with a purely elastic behaviour of the soft soil.

4.4. Column friction angle

The column friction angle has been varied from 35 up to 50° in combination with the dilatancy angle (see Table 3, corresponding values between 0 a 15°). An independent variation of the dilatancy angle has shown to have a negligible influence on the critical length, as has been numerically checked for the reference case (see Figures S1 and S2 of supplementary material). Therefore, it was chosen to vary the dilatancy angle in combination with the friction angle to avoid unrealistic pairs of values, if the friction angle were varied independently (e.g., $\varphi_c = 35°$ and $\psi_c = 10°$ (value for the reference case)).

The results show that an increase in the friction angle of the column reduces the settlement (Fig. 12), and this contribution is more notable in the case of OSC (Fig. 12b) as they are not confined laterally. Regarding the critical column length, it increases with the column friction angle in a similar manner for both OSC and ESC (Fig. 13) because, when the column strength is higher, it takes more load and transfers the load deeper.

4.5. Applied load

Fig. 14 shows the variation of the settlement reduction with the column length for different applied loads, i.e. applied pressures. For ESC (Fig. 14a), the trends are clear and also their interpretation. An increase in the applied pressure causes a deeper extension of the plastic strains and consequently, the critical length increases (Fig. 15), in an analogous manner to a reduction in the soft soil strength (Fig. 11). For $p_{app} = 20$ kPa, the response is mainly elastic (Figure S3 of Supplementary Material), and thus, the corresponding curve in Fig. 14a is smooth without a sharp bend at L_{cr} and a continuous slope after L_{cr}. For OSC, the critical length follows a similar variation (Fig. 15), although this is not so clearly visible in Fig. 14b. The increase of the column critical length with p_{app} is larger in ESC than in OSC, because ESC have more capacity to transmit the load deeper and to produce plastic strains in the soft soil at larger depths.

4.6. Soft soil layer thickness

For floating columns embedded in a deep soft soil layer, the soft soil layer thickness (H) has a negligible influence in practice. In the presented numerical analyses (constant stiffness of the soft soil with depth), the value of the settlement increases with H, and the settlement

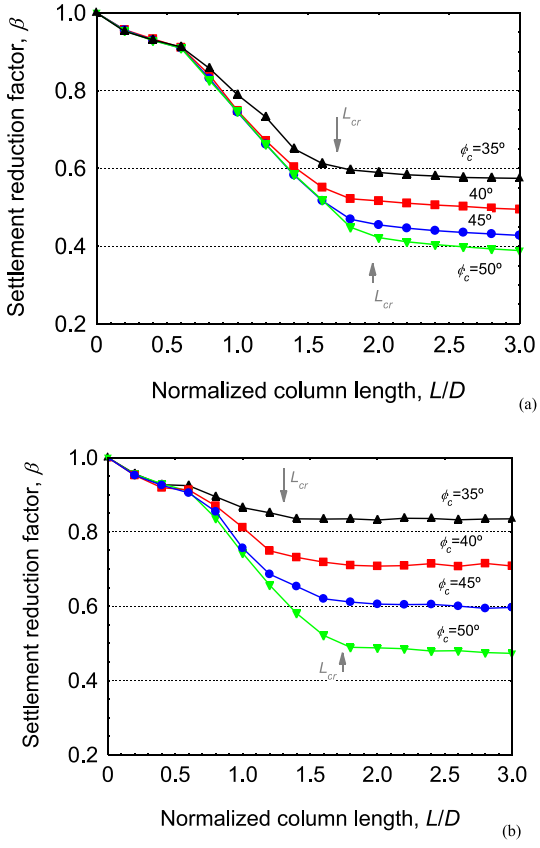

Fig. 12. Variation of the settlement reduction with normalized column length for different column strengths: (a) ESC; (b) OSC.

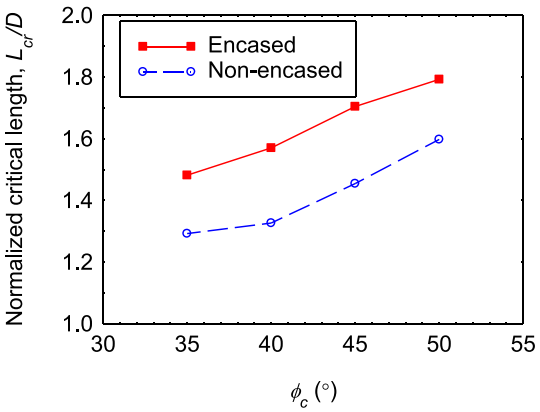

Fig. 13. Critical column length for different column strengths.

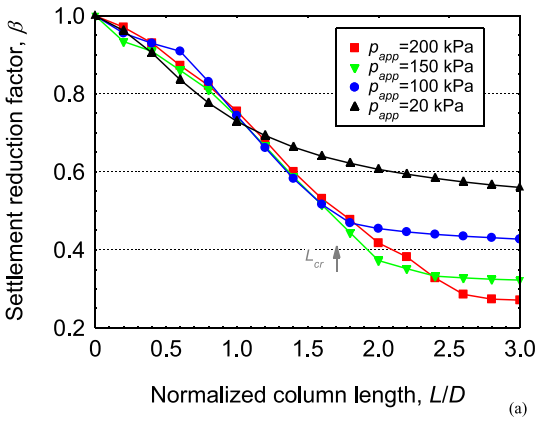

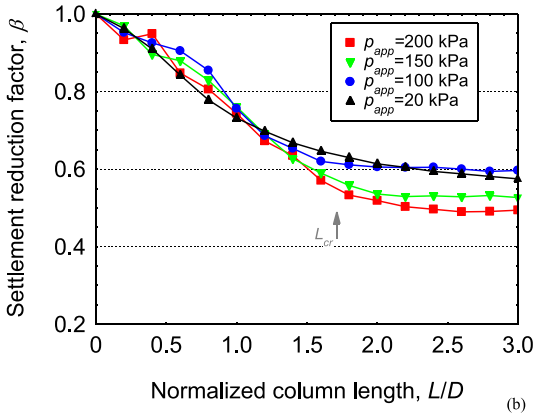

Fig. 14. Variation of the settlement reduction with normalized column length for different applied pressures: (a) ESC; (b) OSC.

reduction factor slightly increases with H (Fig. 16). For those cases, the column critical length remains constant (Fig. 17). Only when H starts to be comparable to the column critical length (e.g., $H/D < 3$), the value of L_{cr} is reduced, and ultimately (e.g., when $H/D < 1.5$) both H and L_{cr} are the same, i.e. $H = L_{cr}$, end-bearing columns.

4.7. Footing diameter

As already mentioned, the area replacement ratio is a key parameter in a stone column treatment (e.g., Castro et al., 2013; Miranda et al., 2015). On the other hand, the influence of the encasement is controlled by its stiffness, or more precisely, by the J_g/d_c ratio. This ratio may be expressed in dimensionless form as $J_g/(E_{ms}d_c)$ (Castro and Sagaseta

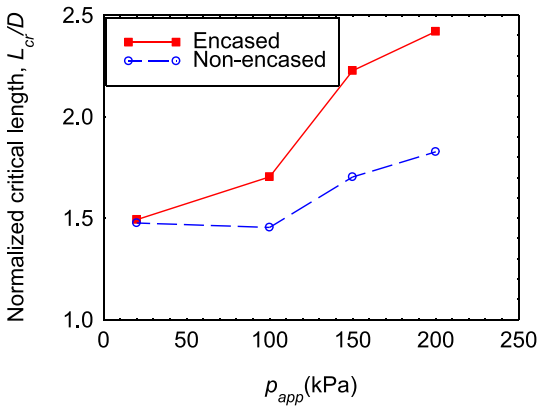

Fig. 15. Critical column length for different applied pressures.

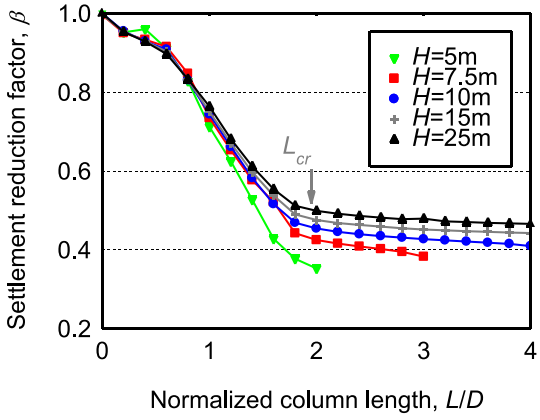

Fig. 16. Variation of the settlement reduction factor with normalized column length for different thicknesses of the soft soil layer. ESC.

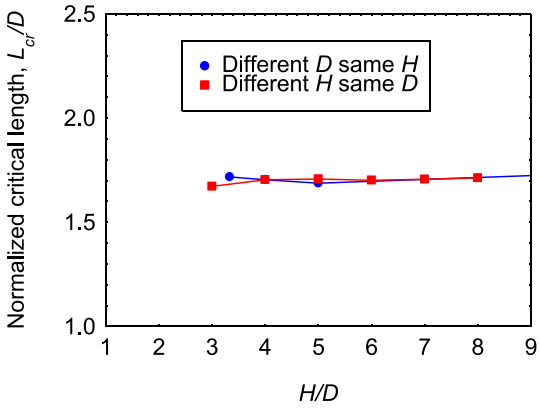

Fig. 17. Critical column length for different thicknesses of the soft layer and footing diameters. ESC.

2013). Besides, the applied load may be normalized as $p_{app}/(\gamma H)$ for end-bearing columns (Castro and Sagaseta 2009). For floating columns (large H/D ratio, e.g., $H/D > 3$), the soft soil layer thickness shall be replaced by the footing dimensions, i.e. $p_{app}/(\gamma D)$.

Here, it was decided not to vary the footing diameter (D) just on its own since it would imply changing the area replacement ratio … but to vary it keeping the above 3 dimensionless parameters constant, namely a_r, J_g/d_c and $p_{app}/(\gamma D)$ (i.e. increasing d_c, J_g and p_{app} for an increase in D). The results are present in Fig. 18. It may be concluded that the normalized critical length (L_{cr}/D) does not change (Fig. 17) and the

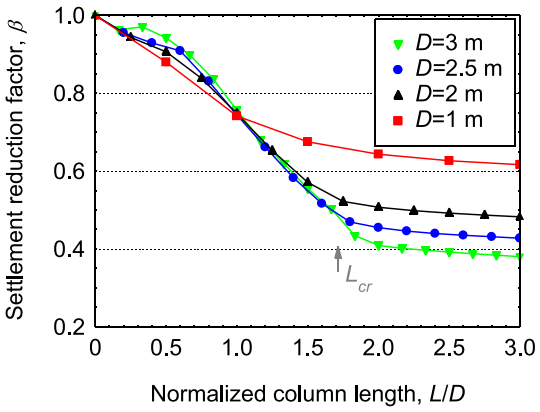

Fig. 18. Variation of the settlement reduction with normalized column length for different footing diameters. ESC.

proposed dimensionless parameters are suitable for presented the analysis.

4.8. Stiffness

The column stiffness was varied between 10 and 80 MPa, but it plays a minor role because the column behavior is mainly plastic. Only for E_c = 10 MPa, the settlement reduction is larger (around 0.58 for ESC) because in that case, the elastic compression of the column is important, but in any case, the column critical length does not notably change (Figure S4 and S5 of Supplementary Material).

On the other hand, soil stiffness has been varied between 0.5 and 5 MPa. Results show that an increase in soil stiffness reduces the settlement reduction factor (Fig. 19), and this trend is more apparent in the case of ESC (Fig. 19a). Critical column length decreases with soil stiffness for both ESC and OSC (Fig. 20). In softer soils, the lateral confinement provided to the column by the surrounding soil is lower, and consequently, the plastic strains develop deeper, and L_{cr} increases.

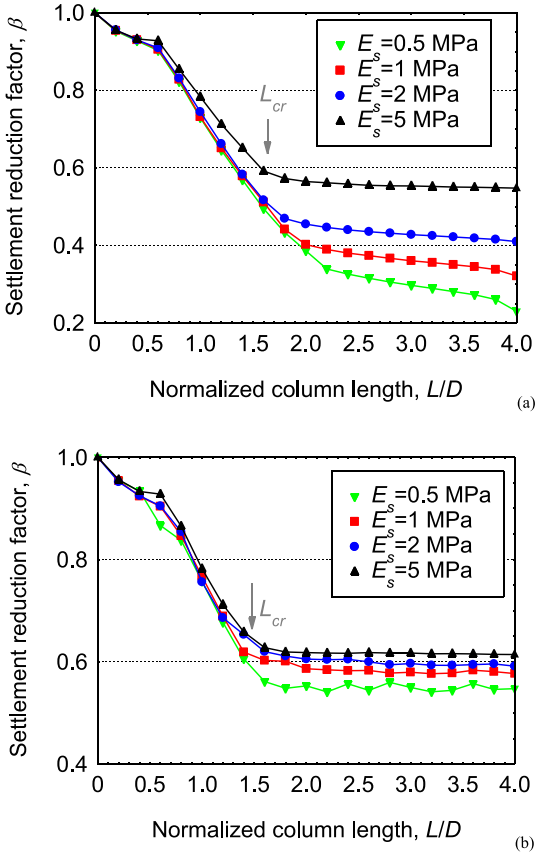

Fig. 19. Variation of the settlement reduction with normalized column length for different soft soil stifnesses: (a) ESC; (b) OSC.

4.9. 3D models

Similar settlement reduction factors were obtained for the 3D models and for the 2D axisymmetric model with an equivalent central column for ESC (Fig. 21). Some differences were found for short columns ($L/D <$ 1). In these cases, the differences are related to the specific location of the column because the equivalent column is in the centre of the footing in the 2D analyses and it mainly acts in the active zone (Fig. 1a). On the contrary, the columns are not just acting in this area for the 3D analyses, but on the radial shear zones as well. Comments above are also valid for OSC (Figure S6 of Supplementary Material).

In any case, the critical column length in the 3D models is approximately the same as in the 2D model (slightly larger in the 2D model because of the central position of the column) (Fig. 22). Therefore, the simplification made by using 2D axisymmetric models is valid to identify trends in the parametric study and to obtain the critical column length with a lower computational effort and in a slightly conservative way.

5. Critical encasement length

So far, the encasement length has been assumed to be equal to the column length, i.e full column encasement $L_g = L$, but some authors proposed to partially encase the columns. For example, Murugesan and Rajagopal (2006) found numerically that it was enough to encase only the upper $2d_c(=2D)$, Muzammil et al. (2018) numerical simulations shows an optimal encasement length for settlement reduction of 6 times the column diameters, while others recommend full column encasement (e.g., Gniel and Bouazza, 2009; Xu et al., 2021; Yoo and Abbas, 2019). Besides, some authors conclude that the optimum encasement length depends on the problem properties, e.g., characteristics of the in situ soft soil and the stiffness of the sleeve (Wu et al., 2009). A particular conclusion was found by Dash and Bora (2013), when studying the influence of partially encasing the columns using small scale laboratory tests, because they found that some partially encased floating columns were superior to the fully encased ones because it produces an enlarged base for the column.

To systematically analyse the critical encasement length, $L_{g,cr}$, numerical analyses are here performed varying both the column and encasement lengths between 2 and 10 m, obviously $L_g \leq L$. Results for the reference case (i.e. a_r = 30% and J = 2 MN/ml) are presented in Fig. 23. For short columns (e.g., L = 2 and 3 m), increasing the encasement length is clearly beneficial until its length is the same as the column length, without a more horizontal part of the settlement

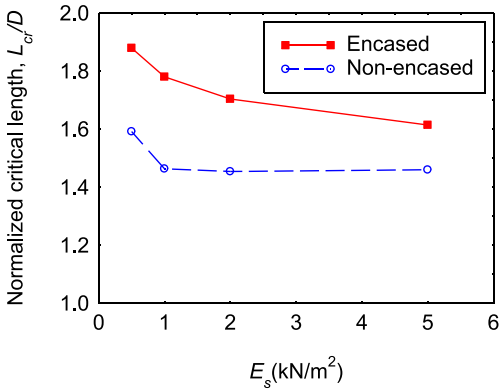

Fig. 20. Critical column length for different soft soil stiffnesses.

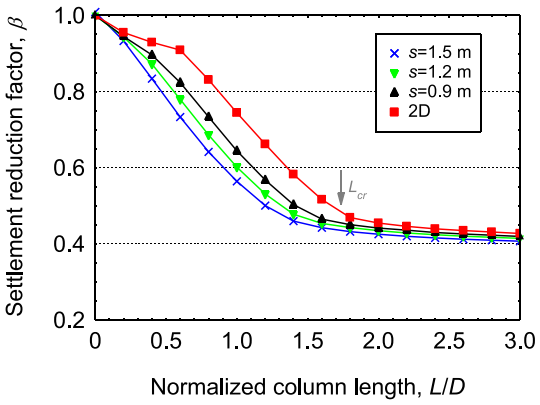

Fig. 21. Settlement reduction factor for the reference 2D model and 3D calculations with different distances between columns. ESC.

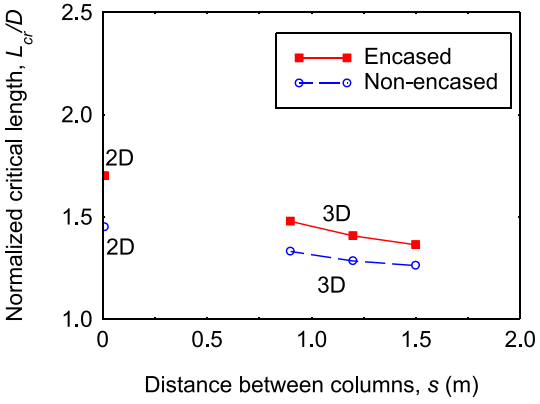

Fig. 22. Critical column length for different column dispositions under the footing.

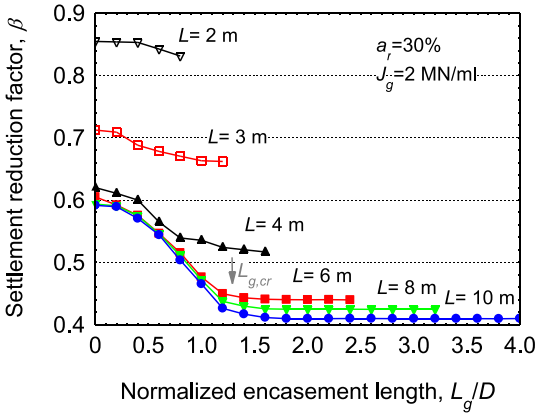

Fig. 23. Variation of settlement reduction with encasement length for different column lengths. Reference case (a_r = 30%, J = 2 MN/ml).

reduction factor vs. encasement length curve. This means that the columns are better fully encased and that the critical encasement length for these cases is equal to the column length ($L_{g,cr} = L$). However, short columns are not recommended because $L < L_{cr}$. For longer columns (e.g., L>4 m in this case), the critical encasement length is no longer the column length, i.e $L_{g,cr} < L$.

Values of the critical encasement length for different area replacement ratios and columns lengths are presented in Fig. 24. The critical encasement length reaches a constant value approximately when $L/D >$ 2.5 for this case. The influence of the encasement stiffness has also been

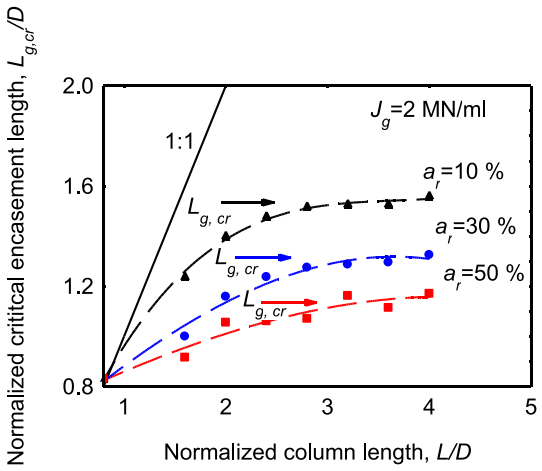

Fig. 24. Critical encasement length for different area replacement ratios.

studied (Figure S7 of Supplementary Material), and similar trends for J = 0.5 and 5 MN/ml are observed. The critical encasement length slightly increases with higher geotextile stiffnesses, as the applied load is transmitted deeper. On the other hand, the critical encasement length reduces with the increment of area replacement ratio (Fig. 24) as a higher part of the load is withstand by the column for higher area replacement ratios reducing the depth where plastic strains develop. Both trends are similar to the ones presented before for the critical column length but values of critical encasement length are slightly lower as presented in Table 4. Therefore, from a theoretical point of view the critical encasement length is slightly lower than the critical column length.

Leaving the column tip without encasement could also contribute to create an enlarge column tip (Dash and Bora, 2013), whose effect has not been considered in the presented numerical simulations. On the other hand, leaving the column tip without encasement has disadvantages for the column construction process and consequently, it is not generally cost-effective. Thus, encasing the full column length is usually the best option. When partial encasement could be calculated as beneficial (e.g. Murugesan and Rajagopal, 2006), it will be more economical in most cases to reduce the whole column length and keep the full encasement of the column.

6. Improvement mechanisms

As explained in Section 2 (Literature review), the pressure bulb (Fig. 1b) is a useful concept to study the critical column length and to justify the dependence of the critical column length on the footing size. However, the pressure bulb is strictly valid only for an elastic behaviour, and the extension of the plastic deformation (Fig. 1c) is better correlated with the critical column length (Castro et al., 2019). Here, this correlation is analysed in detail for ESC, and the conclusions are comparable to those for OSC (Castro et al., 2019).

An analysis of the plastic points for the reference case (Fig. 25) shows 5 different zones: (1a) a small area beneath the footing ($z < 0.24\ D$) where plastic strains are restrained by the footing roughness; (1b) a

Table 4
Values of critical column and encasement length for different area replacement ratios and geotextile encasement stiffnesses.

$L_{cr}/L_{g,cr}$	a_r (%)		
J (MN/ml)	10%	30%	50%
0.5	1.7D/1.4D	1.6 D/1.3D	1.5D/1.1D
2	1.8D/1.5D	1.7D/1.3D	1.6D/1.1D
5	2.0D/1.7D	1.8D/1.3D	1.6D/1.2D

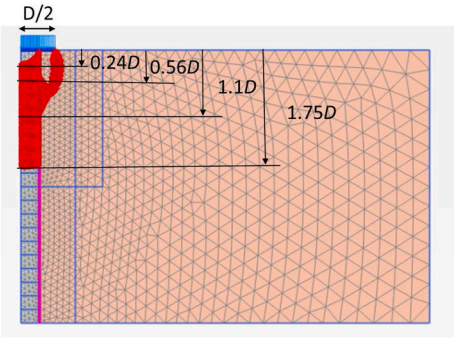

Fig. 25. Plastic points (in red) for the reference case. ESC.

region (z < 0.56 *D*) where the encasement of the column provides enough lateral confinement to the column so that there are not plastic strains in the immediate vicinity of the column; (2) a region (z < 1 *D*) where plastic strains appear in the surrounding soil due to the lack of lateral confinement in the column; (3) a region where plastic strains are just present in the column (z < 1.75 *D*); and (4) a region where there are only elastic strains (z > 1.75*D*).

These five different zones may also be identified in the variation of the settlement reduction factor with the column length (Fig. 26): (1a) the settlement is slightly reduced because the column affects mainly the rigid soil wedge beneath the footing; (1b) a light reduction of the settlement is present as lateral confinement provided by the encasement is getting mobilized and columns still affect mainly the rigid soil wedge; (2) an important reduction of the settlement is visible because plastic strains are reduced both in the soil and column; (3) the settlement is reduced by a smaller amount because the column reduces plastic strains mainly near the column tip; and (4) the reduction of settlement is marginal as the column reduces only elastic strains.

For practical purposes, regions 2, 3 and 4 are the relevant ones. For OSC (Fig. 27 and Fig. 28), region (1b) does not exist, but the regions and the trends are equivalent. For the 3D models, similar results are found (Fig. 29). Only the extension of the plastic points is slightly shorter when the columns are near the footing edges (e.g., s = 1.5m), which is consistent with the slightly shorter values of the critical length for those cases (Fig. 22).

It is worth remarking that a simple linear elastic perfectly plastic model ("Mohr-Coulomb") was used for the soil and the column, and Figs. 25 and 28 show plastic point history, i.e. all the integration (stress) points that have ever been in a plastic state. Similar results are expected when using more advanced models, but in those cases, failure or critical state points should be analysed.

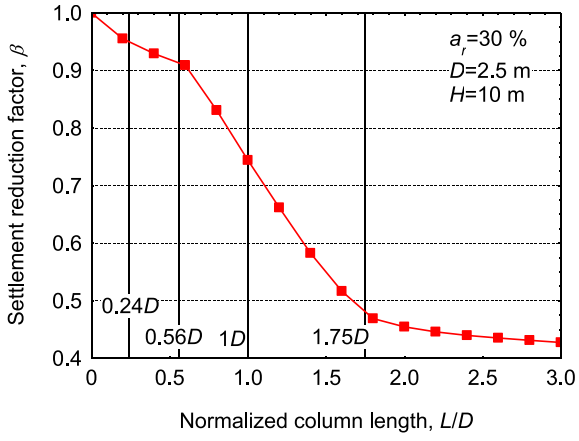

Fig. 26. Settlement reduction factor variation with column length for the different plastic zones of the reference case. ESC.

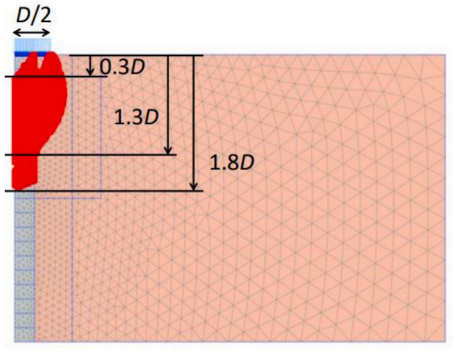

Fig. 27. Plastic points (in red) for the reference case. OSC.

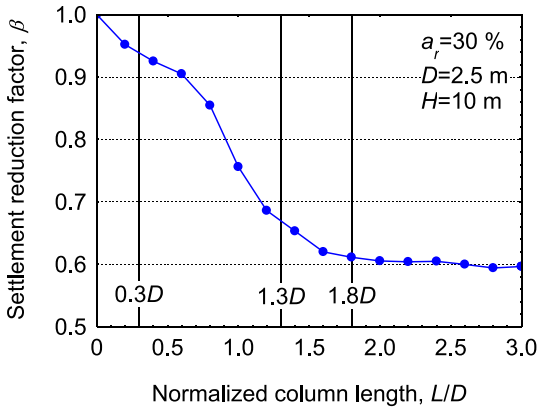

Fig. 28. Settlement reduction factor variation with column length for the different plastic zones of the reference case. OSC.

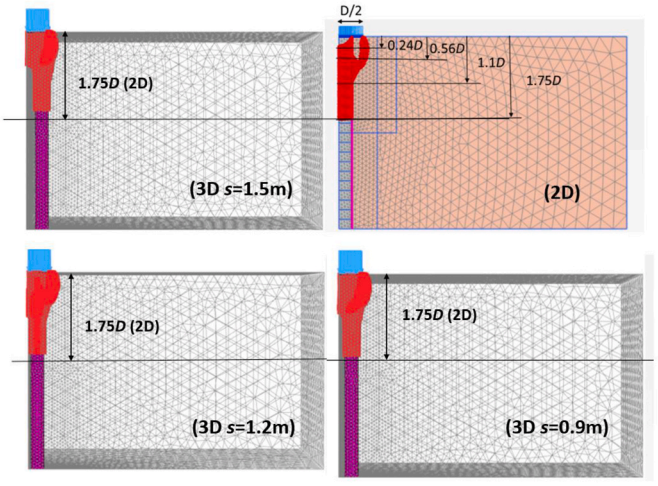

Fig. 29. Plastic points (in red) for the reference case (ESC) in 3D analyses with different spacings between columns and 2D analysis.

Similar results are found for other cases, for example, for twice the footing diameter (D=5 m) (Figures S8, S9, S10 and S11 of Supplementary material). In those cases, the extension of the plastic strains (zones 2 and 3) is reduced due to the proximity of the rigid bedrock, but the correlation between plastic strain zones and the variation of the settlement reduction with the column length is kept. On the other hand, there are some cases where plastic strains are less important and elastic strains play an important role (e.g., p_{app} = 20 kPa in Fig. 14; $\varphi_s = 31°$ in Fig. 10; a_r = 100% in Fig. 6). In these cases, the settlement for zone (4) is

proportionally more important and the slope of the final part of the settlement reduction vs. column length does not look horizontal. However, the absolute value of the settlement caused by those elastic strains is not usually important.

The advantage of considering the plastic zones is that their extension is approximately constant for columns longer than the critical column length. Thus, it is not necessary to perform a parametric analysis varying the length of the columns and it is enough to study the case with end-bearing columns or columns longer than L_{cr} to identify the extension of the plastic zones.

7. Conclusions

This paper presents, for the first time, a systematic analysis of the critical length of ESC and the critical length of their encasement. The analysis is based on parametric numerical simulations and therefore, the conclusions are limited to the studied cases and assumptions (e.g. a unique soft soil layer with constant stiffness). A reanalysis of information available in the literature and the presented numerical analyses show that the critical column length is better expressed as a function of the footing width instead of using the column diameter.

The performed parametric analyses show values of critical column lengths in the range of $L_{cr} = 1.1$ to $1.9D$ for ordinary stone columns and slightly higher values in the case of encased stone columns varying between $L_{cr} = 1.3$ and $2.5D$. Critical column length decreases with the increment of area replacement ratio, the increment of soil strength and the increment of soil stiffness. On the other hand, it reduces when increasing encasement stiffness, strength of material forming the column and applied pressure. Critical length of the encasement $L_{g,cr}$ is found to be slightly lower than the critical column length L_{cr}, for instance, in the range of $L_{g,cr} = 1.1$ to $1.7D$ for a corresponding range of $L_{cr} = 1.5$ to $2.0D$. Thus, in practice it will be usually better from a construction and economical point of view to encase the full column length.

Results from the finite element analyses show that the critical column length is related to the zone where plastic deformations are present. Hence, during the design phase, it could be enough to identify the extent of plastic deformations using finite element analysis in models with longer columns than the L_{cr}. As a first approximation, general values of $L_{cr} = 2D$ and $L_{cr} = 2.5D$ are here proposed for ordinary stone columns and encased stone columns, respectively.

Appendix A. Supplementary data

Supplementary data to this article can be found online at https://doi.org/10.1016/j.geotexmem.2021.05.003.

References

Al Ammari, K., Clarke, B.G., 2018. Effect of vibro stone-column installation on the performance of reinforced soil. J. Geotech. Geoenviron. Eng. 144 (9), 04018056.

Alexiew, D., Raithel, M., 2015. Geotextile-encased columns: case studies over twenty years. In: Indraratna, Chu, Rujikiatkamjorn (Eds.), Embankments with Special Reference to Consolidation and Other Physical Methods. Butterworth-Heinemann, pp. 451–477.

Alkhorshid, N.R., Araujo, G.L., Palmeira, E.M., Zornberg, J.G., 2019. Large-scale load capacity tests on a geosynthetic encased column. Geotext. Geomembranes 47 (5), 632–641.

Almeida, M., Riccio, M., Hosseinpour, I., Alexiew, D., 2019. Geosynthetic Encased Stone Columns for Soft Soil Improvement. CRC Press, Leiden.

Babu, M.R.D., Nayak, S., Shivashankar, R., 2013. A critical review of construction, analysis and behaviour of stone columns. Geotech. Geol. Eng. 31, 1–22.

Barksdale, R.T., Bachus, R.C., 1983. Design and Construction of Stone Columns. Report FHWA/RD-83/026. Nat Tech Information Service, Springfield.

Black, J.A., Sivakumar, V., Bell, A., 2011. The settlement performance of stone column foundations. Geotechnique 61 (11), 909–922.

Bong, T., Stuedlein, A.W., Martin, J., Kim, B.I., 2020. Bearing capacity of spread footings on aggregate pier–reinforced clay: updates and stress concentration. Can. Geotech. J. 57 (5), 717–727.

Brinkgreve, R.B.J., Kumarswamy, S., Swolfs, W.M., Foria, F., 2018. Plaxis 2018 User Manuals. Plaxis bv, Delft.

Brinkgreve, R.B.J., Kumarswamy, S., Swolfs, W.M., Zampich, L., Ragi Manoj, N., 2019. Plaxis 2019 User Manuals. Plaxis bv, Delft.

Castro, J., 2014. Numerical modelling of stone columns beneath a rigid footing. Comput. Geotech. 60, 77–87.

Castro, J., 2016. Discussion of "column supported embankments with geosynthetic encased columns: validity of the unit cell concept". Geotech. Geol. Eng. 34 (1), 419–420.

Castro, J., 2017a. Groups of encased stone columns: influence of column length and arrangement. Geotext. Geomembranes 45, 68–80.

Castro, J., 2017b. Modeling stone columns. Materials 10 (7), 782.

Castro, J., Karstunen, M., 2010. Numerical simulations of stone column installation. Can. Geotech. J. 47 (10), 1127–1138.

Castro, J., Sagaseta, C., 2009. Consolidation around stone columns. Influence of column deformation. Int. J. Numer. Anal. Methods GeoMech. 33 (7), 851–877.

Castro, J., Sagaseta, C., 2013. Influence of elastic strains during plastic deformation of encased stone columns. Geotext. Geomembranes 37, 45–53.

Castro, J., Cimentada, A., da Costa, A., Cañizal, J., Sagaseta, C., 2013. Consolidation and deformation around stone columns: comparison of theoretical and laboratory results. Comput. Geotech. 49, 326–337.

Castro, J., Miranda, M., Da Costa, A., Cañizal, J., Sagaseta, C., 2019. Critical length of stone columns. In: Proceedings of the XVII ECSMGE-2019. 1-7 September 2019, Reykjavik, Iceland.

Cengiz, C., Güler, E., 2018. Seismic behavior of geosynthetic encased columns and ordinary stone columns. Geotext. Geomembranes 46 (1), 40–51.

Dash, S.K., Bora, M.C., 2013. Influence of geosynthetic encasement on the performance of stone columns floating in soft clay. Can. Geotech. J. 50, 754–765.

Ehsaniyamchi, A., Ghazavi, M., 2019. Short-term and long-term behavior of geosynthetic-reinforced stone columns. Soils Found. 59 (5), 1579–1590.

Etezad, M., Hanna, A.M., Khalifa, M., 2018. Bearing capacity of a group of stone columns in soft soil subjected to local or punching shear failures. Int. J. GeoMech. 8 (12), 04018169.

Fleming, K., Weltman, A., Randolph, M., Elson, K., 2009. Piling Engineering, third ed. Taylor and Francis, Oxon.

Gniel, J., Bouazza, A., 2009. Improvement of soft soils using geogrid encased stone columns. Geotext. Geomembranes 27, 167–175.

Han, J., 2015. Principles and Practice of Ground Improvement. Wiley, Hoboken, New Jersey.

Hosseinpour, I., Soriano, C., Almeida, M.S., 2019. A comparative study for the performance of encased granular columns. J. Rock Mech. Geotech. Eng. 11 (2), 379–388.

Hughes, J.M.O., Withers, N.J., 1974. Reinforcing of soft cohesive soils with stone columns. Ground Eng. 7 (3), 42–49.

Keykhosropur, L., Soroush, A., Imam, R., 2012. 3D numerical analyses of geosynthetic encased stone columns. Geotext. Geomembranes 35, 61–68.

King, D.J., Bouazza, A., Gniel, J.R., Rowe, R.K., Bui, H.H., 2018. Geosynthetic reinforced column supported embankments and the role of ground improvement installation effects. Can. Geotech. J. 55 (6), 792–809.

Kirsch, K., Kirsch, F., 2010. Ground Improvement by Deep Vibratory Methods. Spon press, London.

Li, L.Y., Rajesh, S., Chen, J.F., 2020. Centrifuge model tests on the deformation behavior of geosynthetic-encased stone column supported embankment under undrained condition. Geotext. Geomembranes 49 (3), 550–563.

Lima, B.T., Almeida, M.S., Hosseinpour, I., 2019. Field measured and simulated performance of a stone columns-strengthened soft clay deposit. Int. J. Geotech. Eng. 1–10. https://doi.org/10.1080/19386362.2019.1653506.

Malarvizhi, S.N., Ilamparuthi, K., 2007. Comparative study on the behaviour of encased stone column and conventional stone column. Soils Found. 47 (5), 873–885.

McKelvey, D., 2002. The Performance of Vibro Stone Column Reinforced Foundations in Deep Soft Ground. PhD thesis. Queen's University of Belfast.

Miranda, M., Da Costa, A., Castro, J., Sagaseta, C., 2015. Influence of gravel density in the behaviour of soft soils improved with stone columns. Can. Geotech. J. 52 (12), 1968–1980.

Muir Wood, D., Hu, W., Nash, D.F.T., 2000. Group effects in stone column foundations: model tests. Geotechnique 50, 689–698.

Murugesan, S., Rajagopal, K., 2006. Geosynthetic-encased stone columns: numerical evaluation. Geotext. Geomembranes 24 (6), 349–358.

Muzammil, S.P., Varghese, R.M., Joseph, J., 2018. Numerical simulation of the response of geosynthetic encased stone columns under oil storage tank. Int. J. Geosynth. Ground Eng. 4 (1), 1–12.

Nagula, S.S., Nguyen, D.M., Grabe, J., 2018. Numerical modelling and validation of geosynthetic encased columns in soft soils with installation effect. Geotext. Geomembranes 46 (6), 790–800.

Najjar, S.S., Sadek, S., Maakaroun, T., 2010. Effect of sand columns on the undrained load response of soft clays. J. Geotech. Geoenviron. Eng. ASCE 136 (9), 1263–1277.

Ng, K.S., 2017. Settlement ratio of floating stone columns for small and large loaded areas. J. Geo Eng. 12 (2), 89–96.

Ong, D.E.L., Sim, Y.S., Leung, C.F., 2018. Performance of field and numerical back-analysis of floating stone columns in soft clay considering the influence of dilatancy. Int. J. GeoMech. 18 (10), 04018135.

Remadna, A., Benmebarek, S., Benmebarek, N., 2020. Numerical analyses of the optimum length for stone column reinforced foundation. Int. J. Geosynth. Ground Eng. 6 (3), 1–12.

Schnaid, F., Winter, D., Silva, A.E.F., Alexiew, D., Küster, V., 2017. Geotextile encased columns (GEC) used as pressure-relief system. Instrumented bridge abutment case study on soft soil. Geotext. Geomembranes 45 (3), 227–236.

Siahaan, F., Indraratna, B., Ngo, N.T., Rujikiatkamjorn, C., Heitor, A., 2018. Influence of particle gradation and shape on the performance of stone columns in soft clay. Geotech. Test J. 41 (6), 1076–1091.
Soderman, K.L., Giroud, J.P., 1995. Relationships between uniaxial and biaxial stresses and strains in geosynthetics. Geosynth. Int. 2 (2), 495–504.
Tan, S.A., Ng, K.S., Sun, J., 2014. Column group analyses for stone column reinforced foundation. In: From Soil Behavior Fundamentals to Innovations in Geotechnical Engineering: Honoring Roy E. Olson, pp. 597–608.
Wehr, J., 2004. Stone columns – single columns and group behaviour. In: 5th Int. Conf. Ground Improvement Technologies, Kuala Lumpur, pp. 329–340.
Wehr, J., 2006. The undrained cohesion of the soil as criterion for the column installation with a depth vibrator. In: Proceedings of the International Symposium on Vibratory Pile Driving and Deep Soil Vibratory Compaction. TRANSVIB, Paris, pp. 157–162.
Wu, C.-S., Hong, Y.-S., Lin, H.-C., 2009. Axial stress-strain relation of encapsulated granular column. Comput. Geotech. 36, 226–240.
Xu, Z., Zhang, L., Zhou, S., 2021. Influence of encasement length and geosynthetic stiffness on the performance of stone column: 3D DEM-FDM coupled numerical investigation. Comput. Geotech. 132, 103993.
Yoo, C., 2010. Performance of geosynthetic-encased stone columns in embankment construction: numerical investigation. J. Geotech. Geoenviron. Eng. ASCE 136 (8), 36–45.
Yoo, C., Abbas, Q., 2019. Performance of geosynthetic-encased stone column-improved soft clay under vertical cyclic loading. Soils Found. 59 (6), 1875–1890.
Zhou, H., Diao, Y., Zheng, G., Han, J., Jia, R., 2017. Failure modes and bearing capacity of strip footings on soft ground reinforced by floating stone columns. Acta Geotechnica 12, 1089–1103.